Regular Article

PHYSICAL CHEMISTRY RESEARCH
Published by the
Iranian Chemical Society
www.physchemres.org
info@physchemres.org

Phys. Chem. Res., Vol. 6, No. 4, 839-855, December 2018
DOI: 10.22036/pcr.2018.142901.1515

Removal of Zn(II) from Aqueous Solutions Using $NiFe_2O_4$ Coated Sand as an Efficient and Low Cost Adsorbent: Adsorption Isotherm, Kinetic and Thermodynamic Studies

S. Ghaderi[a], F. Moeinpour[b,]* and F.S. Mohseni-Shahri[b]

[a]*Department of Water and Wastewater Engineering, Bandar Abbas Branch, Islamic Azad University, Bandar Abbas, Iran*
[b]*Department of Chemis-try, Bandar Abbas Branch, Islamic Azad University, Bandar Abbas 7915893144, Iran*
(Received 1 August 2018, Accepted 14 October 2018)

In this study, $NiFe_2O_4$ magnetic nanoparticles, as adsorbent for zinc (Zn), were coated on sand particles. Adsorption studies were conducted to investigate the efficacy of contact time, pH, adsorbent dosage, initial zinc ion concentration, and temperature on the removal efficiency. To choose the most fitting kinetic model, the suitability of pseudo-first order and pseudo-second order model was compared and the most appropriate kinetic model was determined to be pseudo-second-order. Langmuir, Freundlich and Dubinin-Radushkevich isotherms were assessed and the most suitable isotherm was observed to be Langmuir model. The maximum adsorption capacity obtained from Langmuir model was 57.14 mg g^{-1}. The calculated thermodynamic parameters indicated the endothermic and spontaneous character of the adsorption process. In addition, the adsorbent can easily be removed by a simple filtration process.

Keywords: Zn(II) removal, Sand, Magnetic nanoparticles, Adsorption, $NiFe_2O_4$

INTRODUCTION

In recent years, pollution of the environment by heavy metals especially some toxic metals has been an attractive subject for scientists due to their increased leakage, toxic nature, non-biodegradable in the environment, and other harmful effects [1]. Zinc is used in many important industrial applications, such as mining, galvanizing plants, pharmaceuticals, paints, pigments, insecticides and fertilizers [2]. In high doses, Zn can be a driving force for many failures such as anemia, dysfunction of pancreas and lungs, metal fume fever, reduced immune functions, growth delay and inhibition, diminished reproduction, dermatitis, sluggishness, and hair loss [3,4]. Based on the World Health Organization, the allowable level for Zn(II) in drinking water is 5 mg l^{-1} [5,6]. So, high level of zinc can cause obvious health problems that must be removed.

Various methods have been used for the treatment and removal of metals from waters and wastewaters including ion exchange, reverse osmosis, chemical precipitation, electro-dialysis, membrane filtration, and electrolysis [7-10]. These methods have some disadvantages, for instance, time consuming, high cost, and secondary waste [11]. The use of nanotechnology is one of the essential methods to solve the deficiencies of above-mentioned methods [10]. Magnetic nanoparticles (NPs) have a great surface area, high adsorption capacity, and rapid adsorption rate. In last years, these unique materials have become more significant due to their particular characteristics. One of their specific characteristics is that almost all the atoms are on the surface of the nanoparticles. So, they can attach to more atoms leading to a superior chemical activity. As a result, the nanoparticles can attract metal ions with a large adsorption rate [12]. Iron oxide-based adsorption is very useful for the adsorption of Zn(II) [13-16]. If the iron-based adsorbent is made in nano-size, it will increase the adsorption efficiency because of higher surface area compared with bulk counterpart. Despite many advantages, the iron based nano-

*Corresponding author. E-mail: f.moeinpour@gmail.com

sized adsorbents have several limitations, for instance, they need external magnetic field to be separated out from the solution after use. A feasible way to overcome the problem of requiring external magnetic field is using filter cartridges, however, this would be an expensive way because of a large quantity of the material needed in the cartridge. So, the immobilization of the iron oxide nano-powder on an inexpensive material such as the sand would be a better way to improve the technique [17]. Ni ferrites ($NiFe_2O_4$) magnetic nanoparticles are among the most multi-purpose magnetic materials with high saturation magnetization, high Curie temperature and chemical stability [18]. In this study, we describe a method to expand an economically adsorbent by coating $NiFe_2O_4$ nanoparticles on sand surface through co-precipitation procedure. The sand is used as a substrate for $NiFe_2O_4$ to provide an inexpensive practical way for removal of poisonous zinc from aqueous solutions. $NiFe_2O_4$-coated nano-adsorbent does not need any external magnetic field for the separation of the adsorbent. For this purpose, nano-adsorbent was synthesized and characterized by various techniques. Then, zinc uptake properties were investigated. Finally, the influence of contact time, pH, adsorbent dosage, initial zinc solution concentration, and temperature on adsorption was examined. Here, by coating the nano-sized $NiFe_2O_4$ adsorbent on the surface of sand particles, the filtration property of the sand has been used that avoids the usage of magnetic field for the separation of $NiFe_2O_4$ nanoparticles.

EXPERIMENTAL

Materials

Ferric nitrate 9-hydrate and nickel nitrate hexahydrate were obtained from Sigma-Aldrich. Hydrochloric acid and nitric acid were purchased from BDH. Analytical-grade salt $Zn(NO_3)_2.6H_2O$ was obtained from Merck, Germany. A 1,000 mg l^{-1} stock solution of the salt was prepared in deionized water.

Analytical Measurements

The crystalline phase of the samples were analyzed using a diffractometer of Philips Company with X'Pert Pro monochromatized Cu Kα radiation (λ = 1.54 Å). The microscopic structures and particle size were examined using SEM (Hitachi S-4800). The concentrations of zinc ions were determined by an atomic absorption spectrophotometer (Varian AA240FS).

Preparation of $NiFe_2O_4$ Nanoparticles on Sand Surface

At first, sand sieved to a geometric average size of 0.6 to 0.9 mm was soaked in an acid solution (1.0 M HCl) for 24 h, which was then washed with distilled water several times and dried at 100 °C temperature. Then, the sand was etched using HNO_3/HCl in the ratio 1:3 for 5 min, and next, it was rinsed to remove the etchant solution.

60 ml of egg white was first mixed with 40 ml deionized water with vigorous stirring at room temperature until a homogeneous solution was obtained. Subsequently, 2.9081 g of $Ni(NO_3)_2.6H_2O$ and 8.0800 g of $Fe(NO_3)_3.9H_2O$ (a mole ratio corresponding to the nominal composition of Ni:Fe ratio of 1:2) and 3.000 g pre-prepared sand were added slowly to the egg white solution with vigorous stirring at room temperature for 2 h to obtain a well-dissolved solution. In all over the process described, no pH adjustment was made. Then, the mixed solution was evaporated by heating on a hot plate at 80 °C with vigorous stirring for several hours until a dried precursor was obtained. To ensure coating the $NiFe_2O_4$ nanoparticles on the surface of sand particles, the coated sand was washed with distilled water up to a clear supernatant was obtained. After filtration, the sand was dried at 85 °C for 3 h. The dried precursor was crushed into powder using a mortar.

Batch Adsorption Experiments

During batch adsorption experiments, the process temperature was set to ~25 °C. 100 ml erlen meyer flasks filled with identified zinc synthetic solutions were utilized at the experiments. The zinc solutions were stirred mechanically during experiments at 250 rpm for an adsorption period of 40 min in the shaker to disperse the adsorbent for a better contact with zinc contaminations. The initial pH values of the solutions were adjusted using relevant amounts of HCl and NaOH. After recovering the adsorbent by filtration, atomic absorption spectrometer (Varian AA240FS) was used to measure the initial and equilibrium zinc concentrations. The research was expanded with parametric studies by gradually changing the values of

several parameters including contact time (5-60 min), initial pH (3-8), adsorbent dosage (0.01-0.5 g/100 ml), initial zinc concentration (5-300 mg l^{-1}) and temperature (20-55 °C). The quantity of zinc adsorbed was calculated by comparing the concentrations in solutions before and after adsorption. Each data point was taken as the average of three measurements. Then, removal efficiency percent (% R) was calculated using Eq. (1) [19]:

$$\%R = \frac{C_0 - C_e}{C_0} \times 100 \quad (1)$$

where C_0 and C_e are the initial and equilibrium zinc concentrations (mg l^{-1}) in solution, respectively.

Adsorption Isotherm Experiments

Adsorption isotherm studies were conducted with 0.1 g/100 ml $NiFe_2O_4$ coated sand nanoparticles and different initial concentrations of zinc. The initial antimony concentration in solution ranged from 5 to 300 mg l^{-1}. The initial pH value of the solution was adjusted to 6.0 with NaOH and HCl. The solution was stirred mechanically on a shaker (250 rpm) for an adsorption period of 40 minutes and 25 °C. Following the equilibrium, the suspensions were separated by filtration to determine the final zinc concentrations.

The most common method used to investigate the adsorption equilibrium data is the adsorption isotherm, describing the concentration adsorbate in the solid phase q as a function of adsorbate concentration in liquid phase C at constant temperature [20].

Two most popular equations, Langmuir and Freundlich isotherm equations, were used for this purpose to fit the equilibrium data, and consequently predict the sorption capacities of the materials used, and identify the mechanism of adsorption. The linear form of the Langmuir equation is presented in Eq. (2) [21]:

$$\frac{1}{q_e} = \frac{1}{K_L} \frac{1}{q_m C_e} + \frac{1}{q_m} \quad (2)$$

where q_e is the amount of Zn(II) adsorbed per unit mass at equilibrium (mg g^{-1}), q_m denotes the maximum amount of adsorbent that can be adsorbed per unit mass adsorbent (mg g^{-1}), C_e is the concentration of adsorbent in the solution at equilibrium (mg l^{-1}) and K_L (l mg^{-1}) represents the Langmuir isotherm constant. A linear plot of $1/q_e$ against $1/C_e$, gives a straight line with a slope of $1/K_L q_m$ and an intercept of $1/q_m$ [21].

The main characteristics of the Langmuir isotherm can be expressed in terms of a dimensionless constant separation factor R_L defined as [22]:

$$R_L = \frac{1}{1 + K_L C_0} \quad (3)$$

where C_0 is the initial concentration of Zn(II) ions (mg l^{-1}), and K_L (l mg^{-1}) is the Langmuir constant. The value of R_L shows the shape of the isotherm to be either unfavorable ($R_L > 1$), linear ($R_L = 1$), favorable ($0 < R_L < 1$), or irreversible ($R_L < 0$).

The Freundlich isotherm is used for heterogeneous adsorption with different surface energy sites and considers the change of uptake with exponential distribution of adsorption sites and energies. The Freundlich model is expressed as follows [23]:

$$\log q_e = \log K_F + \frac{1}{n} \log C_e \quad (4)$$

where q_e is the amount of adsorbent adsorbed per unit mass of adsorbent (mg g^{-1}), C_e denotes the equilibrium concentration of adsorbent in the solution (mg l^{-1}), K_F (mg $1^{-(1/n)}$ $l^{1/n}$ g^{-1}) and n represent Freundlich constants indicating the adsorption capacity for the adsorbent and adsorption intensity, respectively. Freundlich parameters K_F and n can be calculated from the intercept and slope of a linear plot with $\log q_e$ *vs.* $\log C_e$.

The values of n ranging from 1-10 show the chemisorption [24]. Isotherms with $n > 1$ are noticed as L-type isotherms showing a high attraction between the adsorbate and the adsorbent and assigned to the chemisorption [25].

To distinguish between chemical and physical adsorption further, the adsorption data were analyzed using the Dubinin-Radushkevich (D-R) equation defined as:

$$\ln q_e = \ln q_m - \beta\varepsilon^2 \quad (5)$$

where q_m is the maximum adsorption capacity of metal ions (mg g^{-1}), β is a constant related to the mean energy of adsorption (mol^2 kJ^{-2}), and ε is the Polanyi potential given as follows:

$$\varepsilon = RT\ln\left(1+\frac{1}{C_e}\right) \quad (6)$$

where T is the temperature (K) and R is the gas constant (8.314 J K^{-1} mol^{-1}). A linear plot of $\ln q_e$ against ε^2 gives a straight line with a slope of β and an intercept of $\ln q_m$. With the value of β, the mean energy E, which is the free energy transfer of one mole of solute from infinity to the surface of adsorbent, can be evaluated by the following equation:

$$E = \frac{1}{\sqrt{2\beta}} \quad (7)$$

The presumptions of the model are that the adsorption has a multilayer nature, includes van der Waals forces and is appropriate for physical adsorption processes. If E < 8 kJ mol^{-1}, then the adsorption process might be performed physically, but if E > 8 kJ mol^{-1} chemical adsorption may occur [26].

Adsorption Kinetics

The kinetic experiments were carried out to determine the influence of reaction time to reach equilibrium for the adsorption of zinc onto $NiFe_2O_4$ coated sand nanoparticles. By using 100 ml erlen meyer flasks, $NiFe_2O_4$ coated sand nanoparticles with a mass of 0.1 g were added to 100 ml of 20 mg l^{-1} zinc solution (pH = 6). The solution was shaken at 250 rpm during an adsorption period of 60 min. Once the equilibration was achieved, the suspensions were filtered, and all samples were analyzed to determine residual zinc concentration.

Various kinetic models have been proposed and used for precise design of the adsorption process [27]. In this study, the equations of Lagergren's pseudo-first-order kinetic model and Ho's pseudo-second-order kinetic model were applied.

The Pseudo-first order by Lagergren is given as [28]:

$$\ln(q_e - q_t) = \ln q_e - k_1 t \quad (8)$$

where q_e and q_t (mg g^{-1}) are the adsorption capacities at equilibrium and at time t (min) respectively. k_1 (min^{-1}) is the rate constant for the pseudo-first-order model.

The Pseudo-second order equation is defined as [29]:

$$\frac{t}{q_t} = \frac{1}{k_2 q_e^2} + \frac{t}{q_e} \quad (9)$$

where k_2 (g mg^{-1} min^{-1}) is the rate constant for the pseudo-second order rate equation, and other symbols have their usual meanings. The values of q_e and k_2 can be calculated from the slope and intercept of the plot of t/q_t *vs*. t.

RESULTS AND DISCUSSION

Characterization of $NiFe_2O_4$ Nanoparticles Coated Sand Adsorbent

Figure 1 indicates SEM images of $NiFe_2O_4$ nanoparticles, uncoated sand, and coated sand with $NiFe_2O_4$ nanoparticles. The nanoparticles have size less than 100 nm (Fig. 1a). Figure 1b indicates uncoated sand particles; it shows that before coating, the surface of the sand is approximately clear, and after coating is covered with $NiFe_2O_4$ nanoparticles of size less than 100 nm as shown in Fig. 1c.

Figure 2 shows XRD patterns of $NiFe_2O_4$ nanoparticles, uncoated sand, and $NiFe_2O_4$ nanoparticles coated sand, respectively. Figure 2a displays that these nanoparticles have the spinel structure with all the principal peaks corresponding the standard pattern of bulk $NiFe_2O_4$ (JCPDS 08-0234). In the XRD pattern of coated sand (Fig. 2c), most of the peaks are compatible with those of the pure $NiFe_2O_4$ nanoparticles in Fig. 2a, indicating the formation of $NiFe_2O_4$ nanoparticles on the surface of sand. In the case of uncoated sand, sharp and narrow peaks are obtained at different positions corresponding to different faces present in sand as shown in Fig. 2b. Some of the peaks in the XRD pattern of the coated sand correspond to the peaks of uncoated sand.

Effects of Contact Time

The impact of contact time on the Zn(II) adsorption value by $NiFe_2O_4$ coated sand was studied at 20 mg l^{-1} to optimize the adsorption time and to investigate the kinetics of the uptake process. As contact time enhances, the

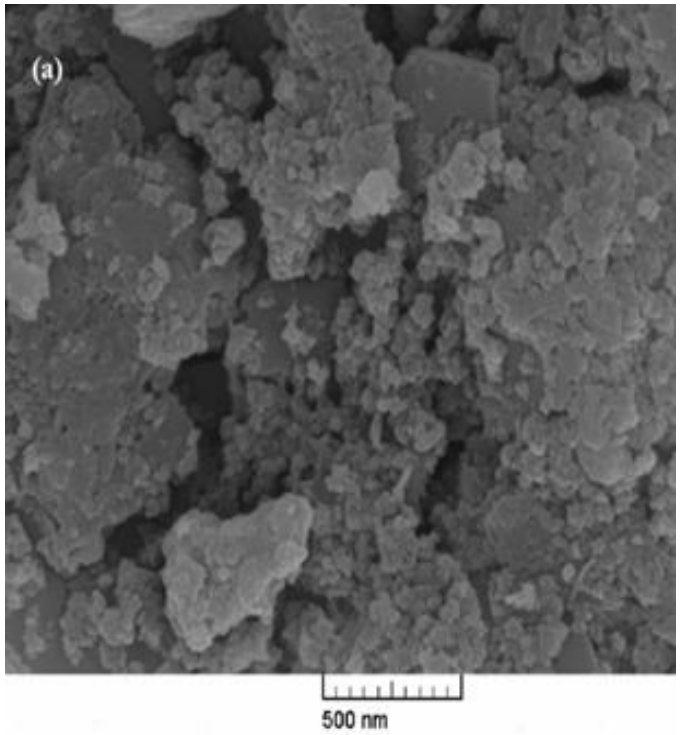

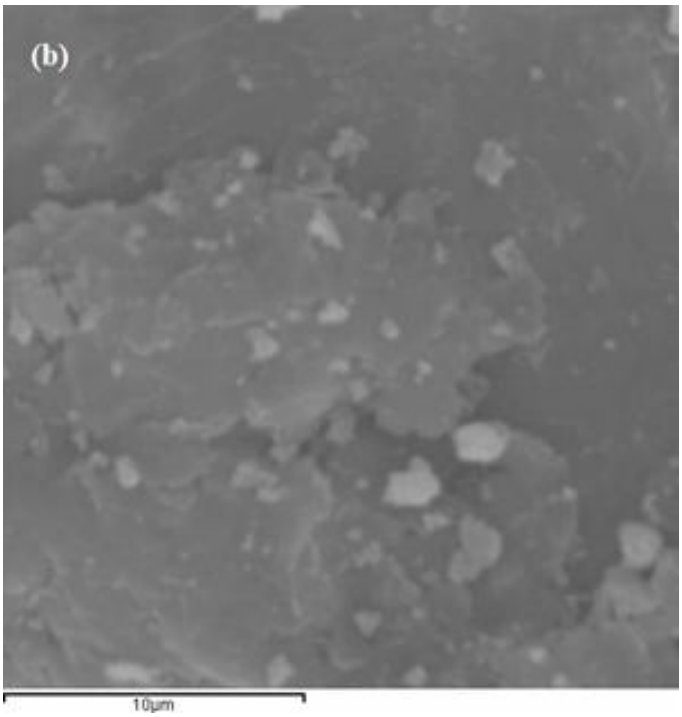

Fig. 1. SEM image of $NiFe_2O_4$ nanoparticles (a), uncoated sand (b) and $NiFe_2O_4$ nanoparticles coated on sand surface (c)

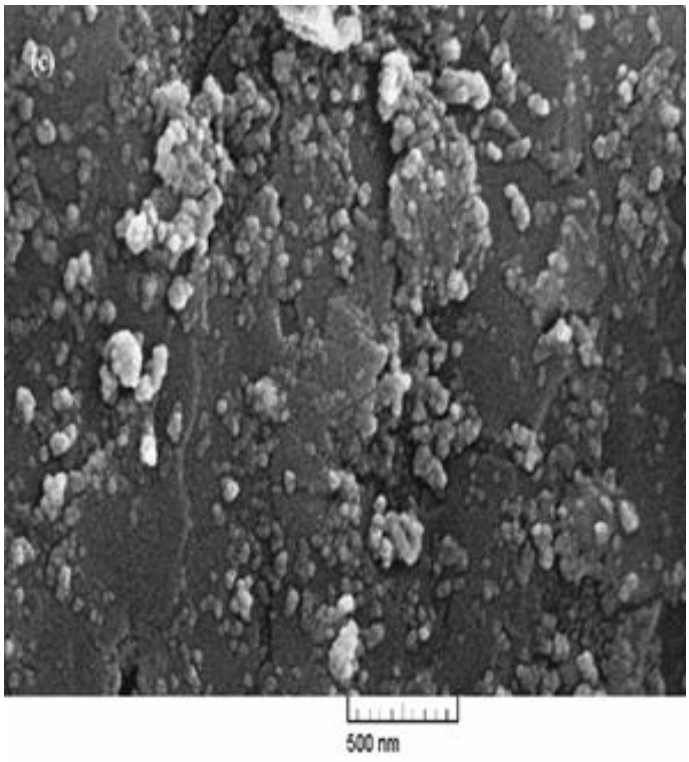

Fig. 1. Continued.

concentration of Zn(II) in the solution reduces quickly at first and later decelerates until remains constant at around 40 minutes, that was taken as the equilibrium time (Fig. 3). This indicates that the removal of Zn(II) by $NiFe_2O_4$ coated sand was very rapid at the beginning. The fast level of Zn(II) adsorption at the early minutes of adsorption process may be due to the great number of empty sites accessible at the early period of the adsorption [30]. The optimum time value was considered to be 40 min. It was reported that a contact time of 60 min was sufficient for Zn(II) removal by activated fruit of Kigelia pinnata [31] and by activated carbon prepared from almond husks [32]. Other researchers reported shorter contact time [33,34] and longer contact times [35,36]. Although the contact time is very important, the uptake efficiency at a certain time depends on the characteristics of adsorbent, temperature, adsorption doses, and other control conditions.

Effect of pH

The acidity of the aqueous solution is one of the most important factors in the adsorption process, especially adsorption capacity [37]. In order to evaluate the influence of pH on the adsorption capacity of adsorbents, the experiments were performed with the pH range of 3-8 (Fig. 4).

The quantity of Zn(II) adsorbed raised with increasing the pH value of solution from 3.0 to 6.0 (approximately) and then with raising the pH value of solution from 6.0 to 8.0 the amount of Zn(II) adsorbed decreased. In these pH values (> 6) the Zn(II) ions begin to hydrolyze and then form a small quantity of zinc hydroxyl species [38]. In other words, at lower pH values (less than 3), the low metal uptake can be assigned to the protonated surfaces of the $NiFe_2O_4$ coated sand, electron repulsion and competition between Zn^{2+} and H^+ ions. For the pH range of 3-6, the equilibrium adsorptions of Zn(II) sharply increased as the pH increased. This behavior can be assigned to lowering the protonation values with the pH increasing that minimize the competition between H^+ and Zn^{2+} on the active sites and increase the Zn(II) values. Additional increment in solution

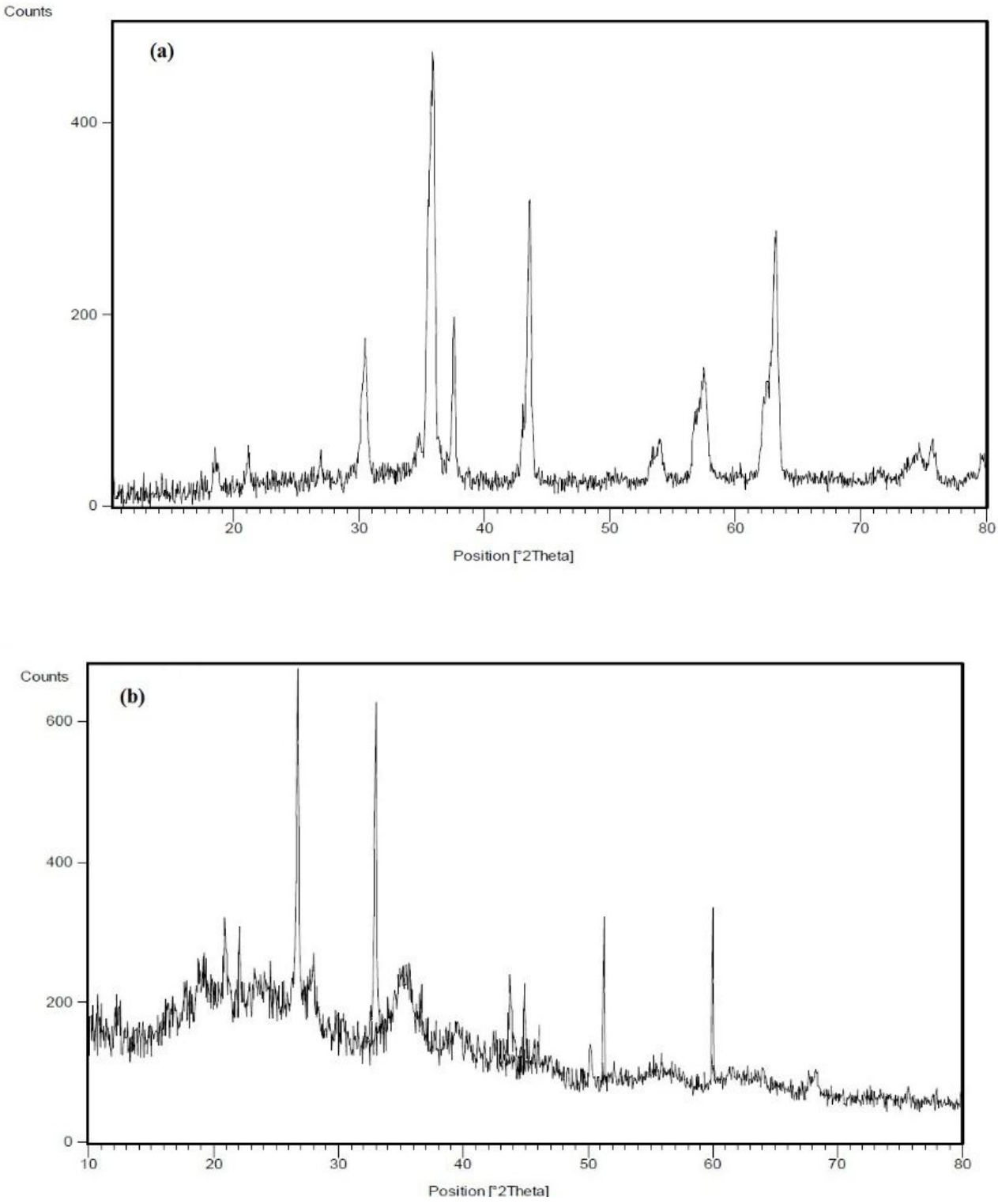

Fig. 2. XRD pattern of $NiFe_2O_4$ nanoparticles (a), uncoated sand (b) and $NiFe_2O_4$ nanoparticles coated sand (c).

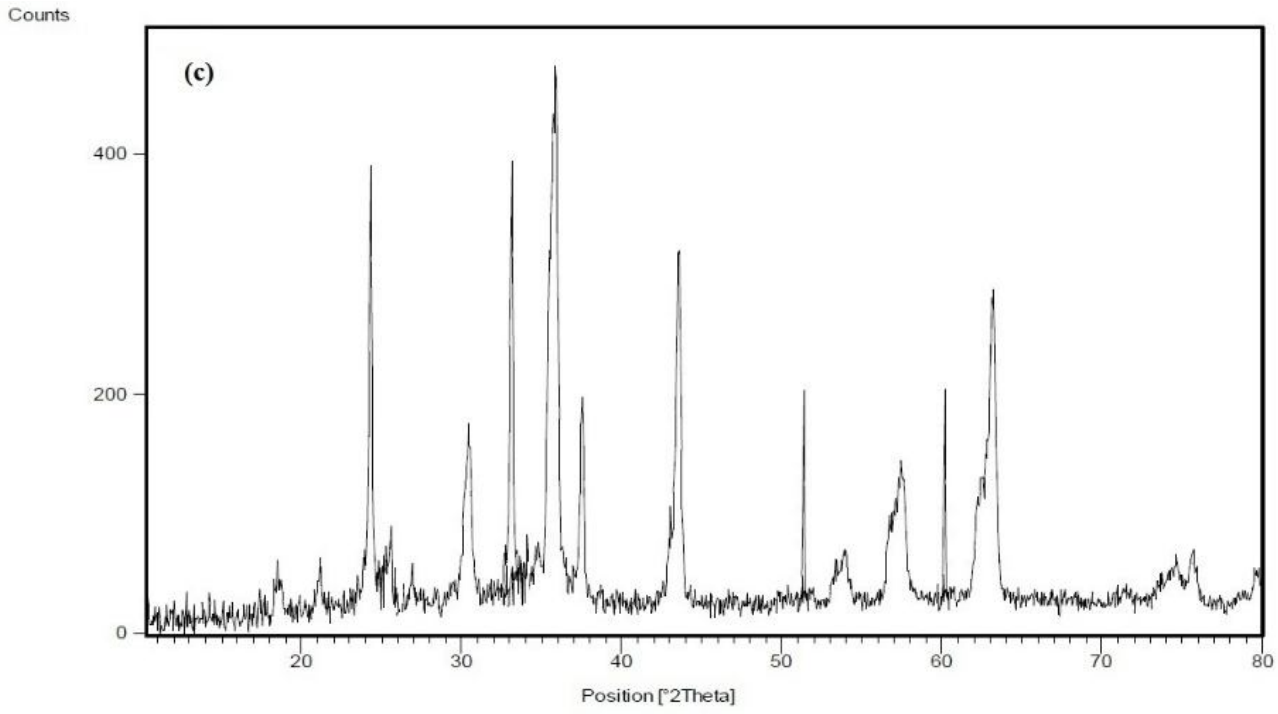

Fig. 2. Continued.

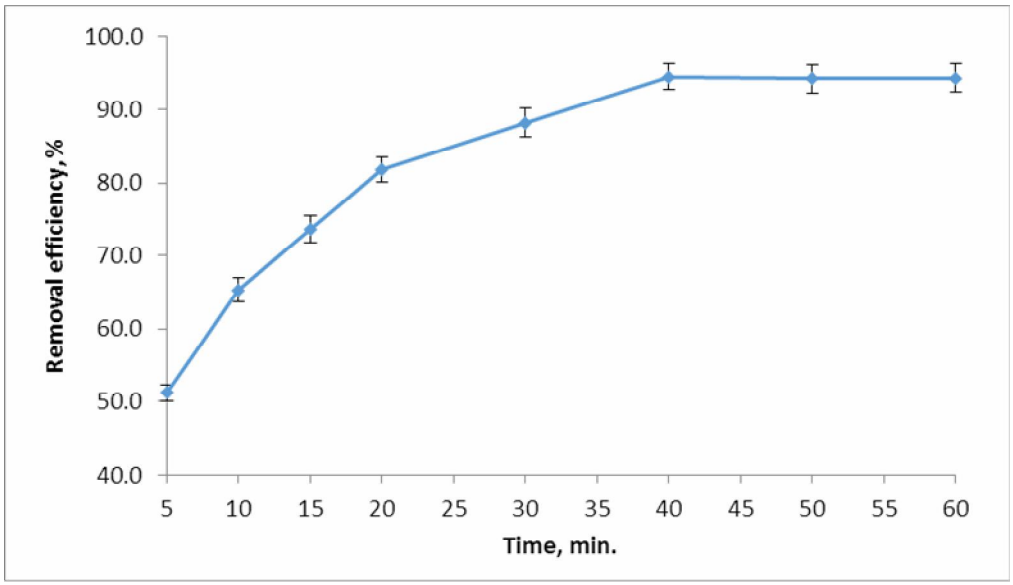

Fig. 3. Effect of contact time on %Zn(II) removal efficiency.

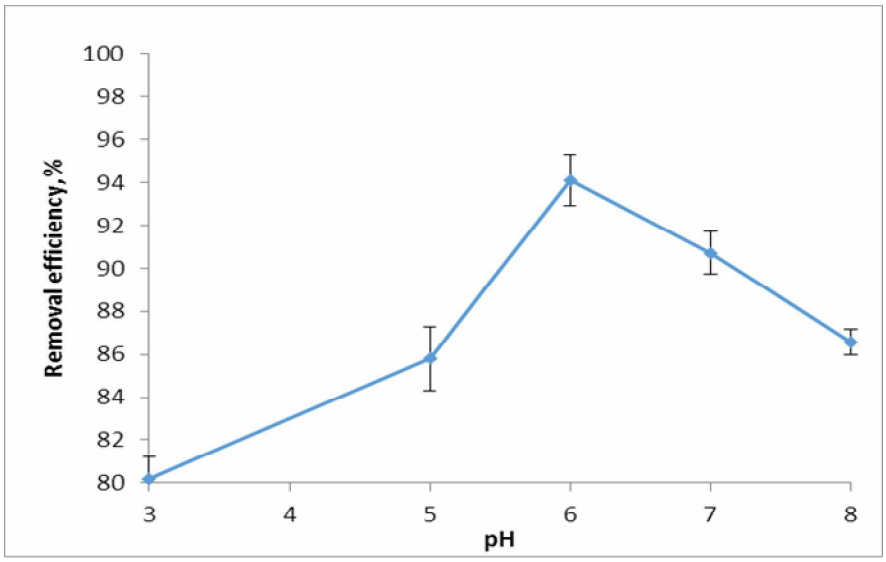

Fig. 4. Effect of pH on %Zn(II) removal efficiency.

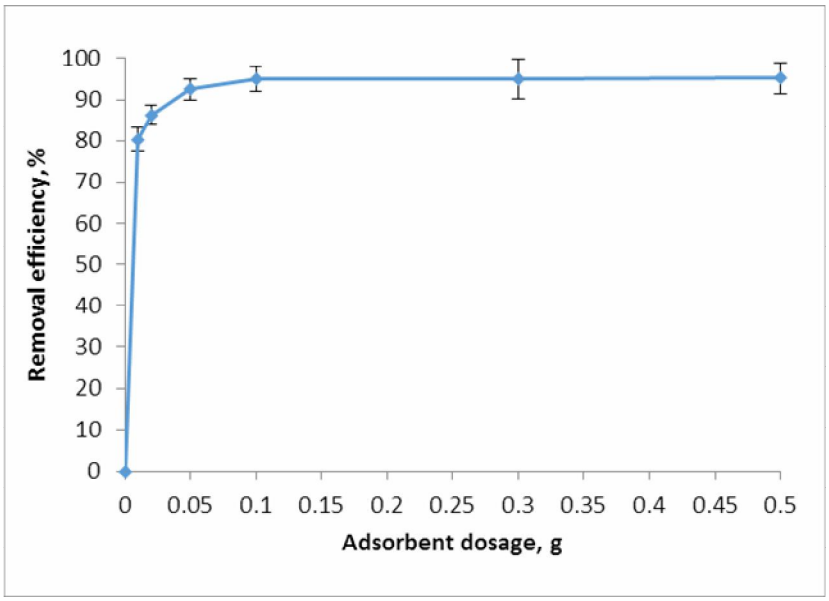

Fig. 5. Effect of adsorbent dosage on %Zn(II) removal efficiency.

pH, beyond 7 brings about precipitation of zinc as zinc hydroxide. In comparison with Zn(II) ions, these species are undesirable for adsorption, which accounts for the small reduction in the percentage of removal efficiency and adsorption capacity. Thus, the maximum adsorption takes place at around pH 6.0 and it is therefore selected for all adsorption experiments in this study. Bayat obtained high Zn(II) removal at a pH of 7 [39]. Others reported lower pH values ranging from 4.2-6.9 [31,34,40] and higher pH values [2]. It is worth mentioning that the optimum pH

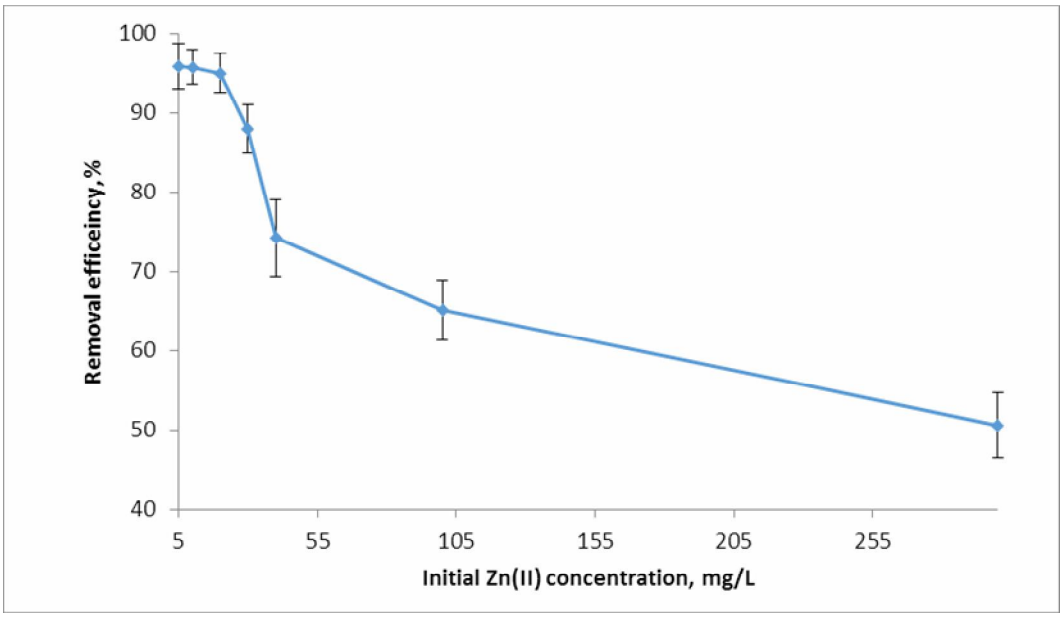

Fig. 6. Effect of initial Zn(II) concentration on %Zn(II) removal efficiency.

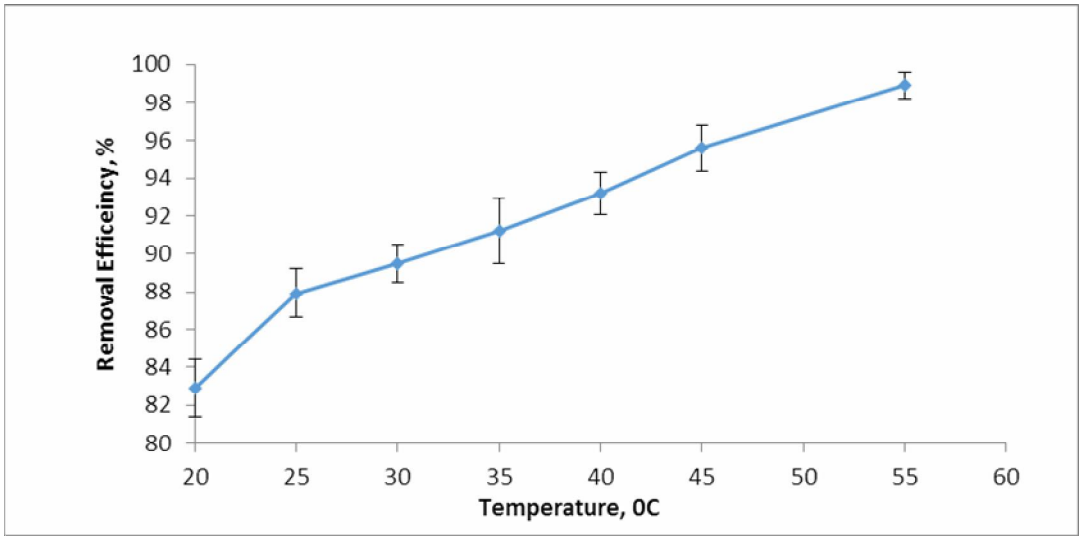

Fig. 7. Effect of temperature on %Zn(II) removal efficiency.

value for metal removal depends on many conditions not limited to the type of adsorbent, adsorption mechanism, and the activation process.

Effect of Adsorbent Dosage

The dependence of adsorption of Zn(II) on adsorbent dose was investigated by varying the quantity of the adsorbent doses in the range of 0.01-0.5 g (Fig. 5).

The outcomes indicate that as the adsorbent dosage rises, the removal percentage of zinc increased, until it approximates to a saturation point where the enhancement in adsorbent dosage does not change the removal

percentage. The increase in Zn(II) removal with increasing adsorbent dosage can be ascribed to enhanced surface area and the adsorption sites. This situation may be clarified with the fact that the higher concentrations of the adsorbent, the more sorbent surface and pore volume will be available for the adsorption. The adsorption reached maximum percentage using 0.1 g of adsorbent. Al-Zboon *et al.* [33] reported that Zn uptake efficiency increased from 52.3 to 97.7% and 98.1% as the adsorbent (natural volcanic tuff-based geopolymer) dose increased from 0.03 to 0.4 and 1 g, respectively.

Effect of Initial Zn(II) Concentration

Batch adsorption tests were carried out at various initial Zn(II) concentrations (5, 10, 20, 30, 40, 100 and 300 mg l^{-1}), at pH 6. 0.1 g l^{-1} of $NiFe_2O_4$ coated sand was used for each adsorption experiment, with a contact time of 40 min. Figure 6 illustrates that with a rise in the initial zinc concentration from 5 to 300 mg l^{-1}, the amount of zinc adsorption decreases. Removal percentage (%R) was greater for low initial Zn(II) concentration owing to accessibility of vacant binding sites on the adsorbent. Since the binding sites were approximately entirely covered at high Zn(II) concentrations, removal efficiency decreased with increasing Zn(II) concentration. Similar result was reported by Al-Zboon *et al.* [33], where the removal efficiency of Zn(II) decreased from 97.8 to 72.5% as the initial concentration increased from 10 to 160 mg l^{-1}, respectively.

Effect of Temperature

Figure 7 indicates the effect of temperature on Zn(II) adsorption, where the adsorption efficiency enhanced linearly with an increment in temperature. To explain the reason for these results, it can be said that with increasing temperature, the mobility and the rate of Zn(II) ions emission in the surface of the adsorbent will increase, which will increase the removal efficiency at higher temperatures.

Adsorption Isotherms

The experimental results of this study were examined by Langmuir, Freundlich and Dubinin-Radushkevich (D-R) models, as shown in Table 1. As the results show, the highest value of R^2 for Langmuir isotherm (0.985) describes that the Zn(II) adsorption on $NiFe_2O_4$ coated sand is best represented by this model. Many researchers confirmed the high validity of Langmuir isotherm model for absorption process [32,36,41]. Based on the Langmuir model, the values of maximum adsorption capacity (q_m) and the Langmuir constant, K_L, for adsorption process were calculated as 57.14 mg g^{-1} and 0.443 l g^{-1}, respectively. The calculated values for R_L are in the range of 0.007-0.311. These values indicated a highly favorable adsorption process ($0 < R_L < 1$) [42]. According to the Freundlich model, the maximum adsorption capacity, K_F, and the value of 1/n that represent the favorability of the adsorption process were calculated as 13.155 and 0.451, respectively. The value of 1/n was less than 0.5, indicating that the adsorption of Zn(II) on $NiFe_2O_4$ coated sand adsorbent was favorable. From Table 1, it is denoted that the predicted q_m value from D-R isotherm is not in agreement with the formerly determined Langmuir isotherm q_m value. The correlation coefficient for the D-R isotherm is the lowest in comparison to those values of other two isotherm models (Table 1), indicating that the Zn(II) uptake on $NiFe_2O_4$ coated sand is not a physical process [43].

Adsorption Kinetics

The kinetics parameters of the pseudo-first and pseudo-second order models are given in Table 2 in which the correlation coefficient value for pseudo-second order model was found to be 0.998 for Zn(II) adsorption by $NiFe_2O_4$ coated sand. In addition, as can be seen in Table 2, the theoretical q_e value from pseudo-second order model is closer to the experimental q_{exp} value. Therefore, the adsorption of Zn(II) on $NiFe_2O_4$ coated sand can be well described by the pseudo-second order kinetic model. Many studies researches proved the validity of the pseudo second-order model for the kinetics of Zn(II) adsorption [44-46].

Thermodynamic study

The thermodynamic parameters such as enthalpy change ($\Delta H°$), free energy change ($\Delta G°$), entropy change ($\Delta S°$) and activation energy (E_a) are the parameters managing the spontaneity of a process. A process will be spontaneous if there is a reduction in $\Delta G°$ value with rising temperature [47]. The temperatures used in the thermodynamic investigation were 293, 298, 303, 308, 313, 318 and 328 K.

Table 1. Langmuir, Freundlich, and D-R Isotherm Constants for the Adsorption of Zn(II) Ions onto $NiFe_2O_4$ Coated Sand

Langmuir			
q_m (mg g^{-1})	K_L	R_L	R^2
57.14	0.443	0.007- 0.311	0.985
Freundlich			
1/n		K_F	R^2
0.451		13.155	0.919
Dubinin-Radushkevich (D-R)			
q_m (mg g^{-1})	B (mol^2 kJ^{-2})	R^2	E (kJ mol^{-1})
126.723	1×10^{-7}	0.633	2.240

Table 2. Kinetic Model Parameters for the Zn(II) Adsorption on $NiFe_2O_4$ Coated Sand

Kinetic models						
Pseudo first-order			Pseudo second-order			
R^2	$q_{e,cal}$ (mg g^{-1})	k_1 (min^{-1})	R^2	q_e,exp. (mg g^{-1})	q_e,cal. (mg g^{-1})	k_2 (g mg^{-1} min^{-1})
0.930	14.918	0.088	0.998	18.981	20.877	0.009

Table 3. Thermodynamic Parameters ΔG, ΔH, ΔS, Ea and S* of Zn(II) Adsorbed on the $NiFe_2O_4$ Coated Sand

T (K)	ΔG° (KJ mol^{-1})	ΔH° (KJ mol^{-1})	ΔS° (KJ mol^{-1} K^{-1})	E_a (KJ mol^{-1})	S^*
293	-3.845	60.416	0.218	56.653	1.696×10^{-11}
298	-4.925				
303	-5.398				
308	-5.988				
313	-6.812				
318	-8.139				
328	-12.281				

Table 4. Maximum Adsorption Capacity of Different Adsorbents for Zn(II) Removal

Adsorbents	Contact time (min)	Langmuir adsorption capacity q_m (mg g^{-1})	Ref.
Amino-functionalized magnetic nanoparticles	90	24 .21	[13]
Mesoporous geopolymeric powder	120	86.00	[53]
Walnut shell treated with citric acid	1200	27.86	[54]
Crab carapace	1440	67.60	[55]
Natural volcanic tuff-Based geopolymer	30	14.70	[33]
Fly ash coated by chitosan	180	55.52	[50]
$NiFe_2O_4$ coated sand	40	57.14	Present study

The thermodynamic parameters were computed on the basis of the following equations:

$$\ln(K_d) = \ln\left(\frac{q_e}{C_e}\right) = \frac{-\Delta G^\circ}{RT} \quad (10)$$

$$\ln(K_d) = \frac{\Delta S^0}{R} - \frac{-\Delta H^\circ}{RT} \quad (11)$$

$$\Delta G° = \Delta H° - T\Delta S° \quad (12)$$

where K_d is the equilibrium constant, q_e is the Zn(II) adsorption capacity at equilibrium (mg g^{-1}), C_e is the concentration of Zn(II) in the solution at equilibrium (mg l^{-1}), T is the solution temperature (K), and R is the gas constant (8.314 J mol^{-1} K^{-1}).

Results are indicated in Table 3. The positive enthalpy change (ΔH°) shows that the adsorption process was endothermic and the value of adsorption supports the formation of partial chemical processes included throughout the removal process [48]. The negative value of the Gibbs free energy change (ΔG°) shows that the adsorption process was spontaneous and the lessening value of ΔG° with raising temperature indicates the spontaneous character of the adsorption of Zn(II) [49]. Fan *et al.* reported that the adsorption of Zn(II) by Penicillium simplicissimum was endothermic and spontaneous in nature [44]. The entropy change ΔS° displays positive value, this verifies that the raising randomness enhances between the solid-solution interfaces during the uptake process.

The sticking probability, S* of an adsorbate on adsorbent can be represented by a modified Arrhenius-type equation related to the surface coverage (θ). S* is a function of the adsorbate/adsorbent system and it is the criterion of an adsorbate capabilityto remain on the adsorbent indefinitely [50], and it is described as:

$$S^* = (1-\theta)e^{\frac{E_g}{RT}} \quad (13)$$

or

$$\ln(1-\theta) = \ln S^* - \frac{E_a}{RT} \quad (14)$$

where θ is surface coverage, E_a is activation energy,

$$\theta = 1 - \frac{C_e}{C_0} \quad (15)$$

and C_0 and C_e are the initial and equilibrium zinc concentrations, respectively. The activation energy and sticking probability are shown in Table 3, from a plot of

ln(1 - θ) *vs*. 1/T (figure not shown). The value of S* was found to be 1.696×10^{-11} that is very close to zero and reveals that adsorption mechanism conforms a chemisorption process [51]. The value of activation energy provides a measure about the type of adsorption that is mostly physical or chemical. Low activation energies (< 40 kJ mol^{-1}) are attributed to the physical uptake, while higher activation energies (>40 kJ mol^{-1}) propose chemical adsorption [52]. The activation energy obtained for the adsorption of Zn(II) on $NiFe_2O_4$ coated sand (56.653 kJ mol^{-1}) shows that the uptake process is chemisorption.

The adsorption capacity is an important parameter that determines the behavior of an adsorbent. Table 4 compares the maximum adsorption capacity of $NiFe_2O_4$ coated sand for Zn(II) adsorption with that of other adsorbents in the literature.

The adsorption capacity of $NiFe_2O_4$ coated sand for Zn(II) ions was found to be 57.14 mg g^{-1}. Table 4 shows that the low cost adsorbents such as amino-functionalized magnetic nanoparticles [13], walnut shell treated with citric acid [54], and natural volcanic tuff-based geopolymer [33] possess Zn(II) adsorption capacity smaller than 50 mg g^{-1}. In addition, most of the low-cost adsorbents require longer time to achieve equilibrium. Mesoporous geopolymeric powder and crab carapace have indicated a capacity of 86.0 and 67.6 mg g^{-1}, respectively, and achieved equilibrium in 120 min and 1440 min, respectively. The results of adsorption of Zn(II) onto $NiFe_2O_4$ coated sand revealed that this material is superior to the low-cost adsorbents reported in the literature because it has higher adsorption capacity requiring lesser time to achieve equilibrium.

CONCLUSIONS

$NiFe_2O_4$ nano-adsorbent has been coated successfully on the surface of sand particles. The functional parameters such as contact time, pH, adsorbent dosage, initial Zn(II) concentration and temperature were found to have an influence on the adsorption efficiency of $NiFe_2O_4$ coated sand. The optimum pH for Zn(II) removal was 6, and the optimum time value was considered to be 40 min. The removal efficiency enhanced when $NiFe_2O_4$ coated sand dosage, contact time, and temperature increased, and initial concentration decreased. The maximum adsorption capacity obtained from Langmuir model was 57.14 mg g^{-1}. The kinetic study shows that the equilibrium is reached within 40 min and fitted well with pseudo-second-order kinetics model rather than pseudo-first-order kinetics model. Adsorption isotherm data is well fitted in Langmuir adsorption isotherm with higher correlation coefficient (R^2 = 0.985). The calculated thermodynamic parameters indicated the endothermic and spontaneous character of the adsorption process. So, the nano-adsorbent $NiFe_2O_4$ coated sand provides an economical and favorable method for the removal of Zn(II) from aqueous solutions.

ACKNOWLEDGEMENTS

The authors acknowledge the Islamic Azad University-Bandar Abbas Branch for financial support of this study.

REFERENCES

[1] Fan, H. -T.; Wu, J. -B.; Fan, X. -L.; Zhang, D. -S.; Su, Z. -J.; Yan, F.; Sun, T., Removal of cadmium(II) and lead(II) from aqueous solution using sulfur-functionalized silica prepared by hydrothermal-assisted grafting method. *Chem. Eng. J.* **2012**, *198*, 355-363, DOI: 10.1016/j.cej.2012.05.109.

[2] Wahi, R.; Kanakaraju, D.; Yusuf, N. A., Preliminary study on zinc removal from aqueous solution by sago wastes. *J. Environ. Res.* **2010**, *4*, 127-134.

[3] Bojic, A. L.; Bojic, D.; Andjelkovic, T., Removal of Cu^{2+} and Zn^{2+} from model wastewaters by spontaneous reduction-coagulation process in flow conditions. *J. Hazard. Mater.* **2009**,*168*, 813-819, DOI: 10.1016/j.jhazmat.2009.02.096.

[4] Liu, Q., Li, Y.; Zhang, J.; Chi, Y.; Ruan, X.; Liu, J.; Qian, G., Effective removal of zinc from aqueous solution by hydrocalumite. *Chem. Eng. J.* **2011**, *175*, 33-38, DOI: 10.1016/j.cej.2011.09.022.

[5] Bhattacharya, A.; Mandal, S.; Das, S., Adsorption of Zn(II) from aqueous solution by using different adsorbents. *Chem. Eng. J.* **2006**, *123*, 43-51, DOI: 10.1016/j.cej.2006.06.012.

[6] Salim, R.; Al-Subu, M.; Abu-Shqair, I.; Braik, H., Removal of zinc from aqueous solutions by dry plant

leaves. *Process Saf. Environ. Prot.* **2003**, *81*, 236-242, DOI: 10.1205/095758203322299752.

[7] Lee, S. -M.; Laldawngliana, C.; Tiwari, D., Iron oxide nano-particles-immobilized-sand material in the treatment of Cu(II), Cd(II) and Pb(II) contaminated waste waters. *Chem. Eng. J.* **2012**, *195*, 103-111, DOI: 10.1016/j.cej.2012.04.075.

[8] Gong, R.; Cai, W.; Li, N.; Chen, J.; Liang, J.; Cao, J., Preparation and application of thiol wheat straw as sorbent for removing mercury ion from aqueous solution. *Desalin. Water Treat.* **2010**, *21*, 274-279, DOI: 10.5004/dwt.2010.1574.

[9] Yogesh Kumar, K.; Muralidhara, H.; Arthoba Nayaka, Y.; Balasubramanyam, J., Low-cost synthesis of mesoporous Zn(II)-Sn(II) mixed oxide nanoparticles for the adsorption of dye and heavy metal ion from aqueous solution. *Desalin. Water Treat.* **2014**, *52*, 4568-4582.

[10] Tang, L.; Yang, G. -D.; Zeng, G. -M.; Cai, Y.; Li, S. -S.; Zhou, Y. -Y.; Pang, Y.; Liu, Y. -Y.; Zhang, Y.; Luna, B., Synergistic effect of iron doped ordered mesoporous carbon on adsorption-coupled reduction of hexavalent chromium and the relative mechanism study. *Chem. Eng. J.* **2014**, *239*, 114-122, DOI: 10.1016/j.cej.2013.10.104.

[11] Wang, Y. -H.; Lin, S. -H.; Juang, R. -S., Removal of heavy metal ions from aqueous solutions using various low-cost adsorbents. *J. Hazard. Mater.* **2003**, *102*, 291-302, DOI: 10.1016/S0304-3894(03)00218-8.

[12] Zhai, Y.; Chang, X.; Cui, Y.; Lian, N.; Lai, S.; Zhen, H.; He, Q., Selective determination of trace mercury(II) after preconcentration with 4-(2-pyridylazo)-resorcinol-modified nanometer-sized SiO_2 particles from sample solutions. *Microchim. Acta* **2006**, *154*, 253-259, DOI: 10.1007/s00604-006-0488-y.

[13] Ghasemi, N.; Ghasemi, M.; Moazeni, S.; Ghasemi, P.; Alharbi, N. S.; Gupta, V. K.; Agarwal, S.; Burakova, I. V.; Tkachev, A. G., Zn(II) removal by amino-functionalized magnetic nanoparticles: Kinetics, isotherm, and thermodynamic aspects of adsorption. *J. Ind. Eng. Chem.* **2018**, *62*, 302-310, DOI: 10.1016/j.jiec.2018.01.008.

[14] Emadi, M.; Shams, E.; Amini, M. K., Removal of zinc from aqueous solutions by magnetite silica core-shell nanoparticles. *J. Chem.* **2012**, 2013, DOI: 10.1155/2013/787682.

[15] Mehdinia, A.; Shegefti, S.; Shemirani, F., Removal of lead(II), copper(II) and zinc(II) ions from aqueous solutions using magnetic amine-functionalized mesoporous silica nanocomposites. *J. Brazil. Chem. Soc.* **2015**, *26*, 2249-2257, DOI: 10.5935/0103-5053.20150211.

[16] Chou, C. -M.; Lien, H. -L., Dendrimer-conjugated magnetic nanoparticles for removal of zinc(II) from aqueous solutions. *J. Nanoparticle Res.* **2011**, *13*, 2099-2107, DOI: 10.1007/s11051-010-9967-5.

[17] Kango, S.; Kumar, R., Low-cost magnetic adsorbent for As(III) removal from water: adsorption kinetics and isotherms. *Environ. Monit. Assess.* **2016**, *188*, 60, DOI: 10.1007/s10661-015-5077-2.

[18] Goldman, A., Modern Ferrite Technology. 2006, Springer Science & Business Media.

[19] Doulia, D.; Leodopoulos, C.; Gimouhopoulos, K.; Rigas, F., Adsorption of humic acid on acid-activated Greek bentonite *J. Colloid Interface Sci.* **2009**, *340*, 131-141.

[20] Ardejani, F. D.; Badii, K.; Limaee, N. Y.; Shafaei, S. Z.; Mirhabibi, A., Adsorption of direct red 80 dye from aqueous solution onto almond shells: Effect of pH, initial concentration and shell type. *J. Hazard. Mater.* **2008**, *151*, 730-737, DOI: 10.1016/j.jhazmat.2007.06.048.

[21] Al-Rashdi, B.; Tizaoui, C.; Hilal, N., Copper removal from aqueous solutions using nano-scale diboron trioxide/titanium dioxide (B_2O_3/TiO_2) adsorbent. *Chem. Eng. J.* **2012**, *183*, 294-302, DOI: 10.1016/j.cej.2011.12.082..

[22] Hall, K. R.; Eagleton, L. C.; Acrivos, A.; Vermeulen T., Pore-and solid-diffusion kinetics in fixed-bed adsorption under constant-pattern conditions. *Ind. Eng. Chem. Fundam.* **1966**, *5*, 212-223, DOI: 10.1021/i160018a011.

[23] Kerkez, Ö.; Bayazit, Ş. S., Magnetite decorated multi-walled carbon nanotubes for removal of toxic dyes from aqueous solutions. *J. Nanoparticle Res.* **2014**, *16*, 2431, DOI: 10.1007/s11051-014-2431-1.

[24] Jiang, J. -Q.; Cooper, C.; Ouki, S., Comparison of

modified montmorillonite adsorbents: part I: preparation, characterization and phenol adsorption. *Chemosphere* **2002**, *47*, 711-716, DOI: 10.1016/S0045-6535(02)00011-5.

[25] Ahmad, K.; Aziz, A. A.; Chik, Z., Geoenvironmental Aspects of Tropical Residual Soils. Tropical Residual Soils Engineering, AA Balkema Publishers London, UK, 2009, 377-403.

[26] Hutson, N. D.; Yang, R. T., Theoretical basis for the Dubinin-Radushkevitch (DR) adsorption isotherm equation. *Adsorption* **1997**, *3*, 189-195, DOI: 10.1007/BF01650130.

[27] Haque, E.; Jun, J. W.; Jhung, S. H., Adsorptive removal of methyl orange and methylene blue from aqueous solution with a metal-organic framework material, iron terephthalate (MOF-235). *J. Hazard. Mater.* **2011**, *185*, 507-511, DOI: 10.1016/j.jhazmat.2010.09.035.

[28] Mostafa, M.; Chen, Y. -H.; Jean, J. -S.; Liu, C. -C.; Lee, Y. -C., Kinetics and mechanism of arsenate removal by nanosized iron oxide-coated perlite. *J. Hazard. Mater.* **2011**, *187*, 89-95, DOI: 10.1016/j.jhazmat.2010.12.117.

[29] Khorzughy, S. H.; Eslamkish, T.; Ardejani, F. D.; Heydartaemeh, M. R., Admium removal from aqueous solutions by pumice and nano-pumice. *Korean J. Chem. Eng.* **2015**, *32*, 88-96, DOI: 10.1007/s11814-014-0168-2.

[30] Yousef, R. I.; El-Eswed, B.; Ala'a, H., Adsorption characteristics of natural zeolites as solid adsorbents for phenol removal from aqueous solutions: kinetics, mechanism, and thermodynamics studies. *Chem. Eng. J.* **2011**, *171*, 1143-1149, DOI: 10.1016/j.cej.2011.05.012.

[31] Sahayaraj, P. A.; Dharmalingam, V.; Soruba, R., Adsorption study on zinc(II) ions from aqueous solution using chemically activated fruit of kigelia pinnata (JACQ) DC carbon. *Int. Reser. J. Env. Sci.* **2014**, *3*, 65-69.

[32] Hasar, H.; Cuci, Y.; Obek, E.; Dilekoglu, M. F., Removal of zinc(II) by activated carbon prepared from almond husks under different conditions. *Adsorpt. Sci. Technol.,* **2003**, *21*, 799-808, DOI: 10.1260/02636170360744056.

[33] Al-Zboon, K. K.; Al-smadi, B. M.; Al-Khawaldh, S., Natural volcanic tuff-based geopolymer for Zn removal: adsorption isotherm, kinetic, and thermodynamic study. *Water Air Soil Pollut.* **2016**, *227*, 248, DOI: 10.1007/s11270-016-2937-5.

[34] Saeed, A.; Akhter, M. W.; Iqbal, M., Removal and recovery of heavy metals from aqueous solution using papaya wood as a new biosorbent. *Sep. Purif. Technol.* **2005**, *45*, 25-31, DOI: 10.1016/j.seppur.2005.02.004.

[35] Wasewar, K. L.; Prasad, B.; Atif, M., Characterization of tea factory waste as an adsorbent. *J. Future Eng. Technol.* **2008**, *3*, 49-55.

[36] Sampranpiboon, P.; Charnkeitkong, P.; Feng, X., Equilibrium isotherm models for adsorption of zinc (II) ion from aqueous solution on pulp waste. *WSEAS Trans. Environ. Develop.* **2014**, *10*, 35-47.

[37] Omidvar-Hosseini, F.; Moeinpour, F., Removal of Pb(II) from aqueous solutions using Acacia Nilotica seed shell ash supported $Ni_{0.5}Zn_{0.5}Fe_2O_4$ magnetic nanoparticles. *J. Water Reuse Desal.* **2016**, *6*, 562-573, DOI: 10.2166/wrd.2016.0.

[38] Kaya, A.; Ören, A. H., Adsorption of zinc from aqueous solutions to bentonite. *J. Hazard. Mater.* **2005**, *125*, 183-189, DOI: 10.1016/j.jhazmat.2005.05.027.

[39] Bayat, B., Combined removal of zinc(II) and cadmium(II) from aqueous solutions by adsorption onto high-calcium Turkish fly ash. *Water Air Soil Pollut.* **2002**, *136*, 69-92, DOI: 10.1023/A:10152960.

[40] Wasewar, K. L.; Kailas L. A.; Atif, M.; Prasad, B.; Mishra, I. M., Batch adsorption of zinc on tea factory waste. *Desalination* **2009**, *244*, 66-71, DOI: 10.1016/j.desal.2008.04.036.

[41] Meroufel, B., Benali, O.; Benyahya, M.; Zenasni, M., Merlin, A.; George, B., Removal of Zn(II) from aqueous solution onto kaolin by batch design. *J. Water Res. Protec.* **2013**, *5*, 669-680, DOI: 10.4236/jwarp.2013.57067.

[42] Dada, A.; Olalekan, A.; Olatunya, A.; Dada, O., Langmuir, Freundlich, Temkin and Dubinin-Radushkevich isotherms studies of equilibrium sorption of Zn^{2+} unto phosphoric acid modified rice husk. *IOSR J. Appl. Chem.* **2012**, *3*, 38-45, DOI:

10.9790/5736-0313845.

[43] Boparai, H. K.; Joseph, M.; O'Carroll, D. M., Kinetics and thermodynamics of cadmium ion removal by adsorption onto nano zerovalent iron particles. *J. Hazard. Mater.* **2011**, *186*, 458-465, DOI: 10.1016/j.jhazmat.2010.11.029.

[44] Fan, T., Liu, Y.; Feng, B.; Zeng, G.; Yang, C.; Zhou, M.; Zhou, H.; Tan, Z.; Wang, X., Biosorption of cadmium(II), zinc(II) and lead(II) by Penicillium simplicissimum: Isotherms, kinetics and thermodynamics. *J. Hazard. Mater.* **2008**, *160*, 655-661, DOI: 10.1016/j.jhazmat.2008.03.038.

[45] Ozdemir, G.; Ceyhan, N.; Ozturk, T.; Akirmak, F.; Cosar, T., Biosorption of chromium(VI), cadmium(II) and copper(II) by Pantoea sp. TEM18. *Chem. Eng. J.* **2004**, *102*, 249-253, DOI: 10.1016/j.cej.2004.01.032.

[46] Liu, Y. -G., Ting, F.; Zeng, G. -M.; Xin, L.; Qing, T.; Fei, Y.; Ming, Z.; Xu, W. -H.; Huang, Y., Removal of cadmium and zinc ions from aqueous solution by living Aspergillus niger. *Trans. Nonferrous Met. Soc. China* **2006**, *16*, 681-686, DOI: 10.1016/S1003-6326(06)60121-0.

[47] Ngah, W. W.; Hanafiah, M., Adsorption of copper on rubber (Hevea brasiliensis) leaf powder: Kinetic, equilibrium and thermodynamic studies. *Biochem. Eng. J.* **2008**, *39*, 521-530, DOI: 10.1016/j.bej.2007.11.006.

[48] Kumar, M.; Tamilarasan, R.; Sivakumar, V., Adsorption of Victoria blue by carbon/Ba/alginate beads: Kinetics, thermodynamics and isotherm studies. *Carbohyd. Polym.* **2013**, *98*, 505-513, DOI: 10.1016/j.carbpol.2013.05.078.

[49] Zou, W.; Li, K.; Bai, H.; Shi, X.; Han, R., Enhanced cationic dyes removal from aqueous solution by oxalic acid modified rice husk. *J. Chem. Eng. Data* **2011**, *56*, 1882-1891, DOI: 10.1021/je100893h.

[50] Adamczuk, A.; Kołodyńska, D., Equilibrium, thermodynamic and kinetic studies on removal of chromium, copper, zinc and arsenic from aqueous solutions onto fly ash coated by chitosan. *Chem. Eng. J.* **2015**, *274*, 200-212, DOI: 10.1016/j.cej.2015.03.088.

[51] Horsfall Jnr, M.; Spiff, A. I., Effects of temperature on the sorption of Pb^{2+} and Cd^{2+} from aqueous solution by Caladium bicolor (Wild Cocoyam) biomass. *Electron. J. Biotechn.* **2005**, *8*, 43-50, DOI: 10.4067/S0717-34582005000200005.

[52] Chakraborty, S.; Chowdhury, S.; Saha, P. D., Adsorption of crystal violet from aqueous solution onto NaOH-modified rice husk. *Carbohyd. Polym.* **2011**, *86*, 1533-1541, DOI: 10.1016/j.carbpol.2011.06.058.

[53] Sarkar, C.; Basu, J. K.; Samanta, A. N., Synthesis of mesoporous geopolymeric powder from LD slag as superior adsorbent for Zinc(II) removal. *Adv. Powder Technol.* **2018**, *29*, 1142-1152, DOI: 10.1016/j.apt.2018.02.005.

[54] Segovia-Sandoval, S. J.; Ocampo-Pérez, R.; Berber-Mendoza, M. S.; Leyva-Ramos, R.; Jacobo-Azuara, A.; Medellín-Castillo, N. A., Walnut shell treated with citric acid and its application as biosorbent in the removal of Zn(II). J. Water Process *Eng.* **2018**, *25*, 45-53, DOI: 10.1016/j.jwpe.2018.06.007.

[55] Lu, S.; Gibb, S. W.; Cochrane, E., Effective removal of zinc ions from aqueous solutions using crab carapace biosorbent. *J. Hazard. Mater.* **2007**, *149*, 208-217, DOI: 10.1016/j.jhazmat.2007.03.070.